



# Short-range Forecasting Research

Short Range Forecasting Division  
Scientific Paper No. 11

## A NEW APPROACH TO SHALLOW FLOW OVER AN OBSTACLE

### I General Theory

by

A.S. Broad, D. Porter and M.J. Sewell

10 August 1992

Meteorological Office  
London Road  
Bracknell  
Berkshire  
RG12 2SZ  
United Kingdom

ORGS UKMO S

National Meteorological Library  
FitzRoy Road, Exeter, Devon. EX1 3PB

A NEW APPROACH TO SHALLOW FLOW OVER AN OBSTACLE

I General Theory

by

A.S. Broad

Meteorological Office, Bracknell, RG12 2SZ

D. Porter and M.J. Sewell

Department of Mathematics, University of Reading,

Whiteknights, Reading RG6 2AX

10 August 1992

Abstract

A novel approach to the study of shallow flow of water over an uneven bed, and of air over mountains, is initiated. Generality is achieved via the concept of constitutive surfaces, which are geometrical expressions of particle properties valid in any motion whatever. Connections are made with the cusp and swallowtail catastrophes. The various types of bores which can travel over an uneven surface are classified. General local formulae which express the solutions of the balance conditions of mass and momentum at a bore or hydraulic jump are derived.

1. Introduction

The objective of these papers is to initiate and develop a new approach to the study of shallow flow over obstacles. This will apply to the flow of air over mountains, and to water over an uneven bed. A number of papers have been written in this area, to which we shall refer later where appropriate. The present approach subsumes and considerably extends the existing literature. Given the limitations of shallow water theory, which are well understood, we show that it can be used to provide a very precise study of the mechanics, for example of the local properties of bores over an uneven bed extending in two dimensions, in a generality not previously attempted. We give a strong emphasis to geometrical properties of the theory.

The novelty of the approach is that it is based on the concept of the constitutive surface, which was introduced into gas dynamics and shallow water theory by Sewell and Porter (1980). This is a property of each particle, in any motion whatever, and therefore has a basic role allowing one to deduce results which are equally valid in motion which is steady or unsteady, in one, two or three dimensions, with or without rotation of the bed, and whether discontinuities such as shocks and bores are present or not. Furthermore, there proves to be a close connection between the shapes of constitutive surfaces and the cusp and swallowtail catastrophes, via the notion of Legendre duality (Sewell, 1987).

Part I shows how to adapt the notion of the constitutive surface to shallow flow over an uneven rigid bed extending over two dimensions, in §3. We thus derive a number of quite general properties of unsteady shallow water theory. Appropriate balance equations of mass, momentum

and energy are given in §4. Rotation of the bed is allowed for, as some geophysical applications will require. A classification of the various types of bores (perhaps curved in plan view) which can travel over a bumpy plane is given in §5. General local formulae which solve the jump conditions of balance are obtained, for example to express the energy dissipation at the bore, and the bore speed, in terms of the strength of the bore. A new swallowtail interpretation is given to a general hydraulic jump, and extended to bores.

We take the view that a thorough understanding of the variety of possible local events which we reveal here is a desirable prerequisite to the fitting of any particular set of conditions at a distance.

Part II applies this general theory to a one dimensional case, i.e. in which the shallow flow is the same in every parallel vertical plane, and there is a single obstacle perpendicular to that plane. We consider a wide family of obstacle profiles, and demonstrate new pseudo-steady flows over them which include smooth bifurcations at the obstacle top when the latter is locally non-parabolic, and bores running upstream from the obstacle. Many new results are given. For example, such bores can convert a blocked flow not only into a subcritical free flow, but also into a subcritical flow which can then bifurcate at the top into either a supercritical or a subcritical flow as far as local conditions can determine. A sensitivity of the free surface shape to that of the obstacle profile is demonstrated. We have not seen this sensitivity remarked upon elsewhere.

We begin in §2 by recalling those standard features of shallow water theory upon which the subsequent new material is based.

## 2. Shallow Water Theory

We consider an incompressible inviscid fluid of uniform density  $\rho$  flowing in a region spanned by a fixed system of cartesian coordinates  $x_1, x_2, x_3$ , where  $x_3$  is measured vertically upwards. The flow takes place between a rigid bed  $x_3 = b(x_1, x_2)$  and an upper surface  $x_3 = s(x_1, x_2, t)$ , where  $t$  denotes time. The function  $b(x_1, x_2)$  is given and piecewise  $C^1$ , but the function  $s(x_1, x_2, t)$  is unknown in advance. Let

$$d = s - b > 0 \tag{1}$$

denote the total fluid depth, which will also be an unknown function  $d(x_1, x_2, t)$ .

The fluid may be air flowing over mountains, or water over an uneven bottom. The bed may be fixed, or rotating when the spin of the earth is locally important.

Let  $\bar{p}$  denote the true pressure, which is a function of  $x_1, x_2, x_3, t$ . Assume that vertical momentum balance is satisfied by the hydrostatic approximation  $\partial \bar{p} / \partial x_3 + \rho g = 0$ , with constant  $g > 0$ . We choose the upper surface to be free in the sense that  $\bar{p} = 0$  there, and so obtain  $\bar{p} = \rho g (s - x_3)$ . Let  $p > 0$  be a new variable such that, at any given horizontal station  $x_1, x_2$  at time  $t$ , the vertically averaged pressure

$$\int_b^s \bar{p} \, dx_3 = \rho p . \tag{2}$$

It follows that

$$p = \frac{1}{2} g d^2 \quad (3)$$

so that  $p(x_1, x_2, t)$  is a function of the horizontal station and time which is also unknown in advance.

There are several ways of scaling the variables to write (3) as the parabola  $y = \frac{1}{2} x^2$ , such as  $p/g = \frac{1}{2} d^2$  or  $pg = \frac{1}{2} (gd)^2$ . We could have eliminated further mention of  $g$ , like  $\rho$ , by writing  $\rho gp$  on the right of (2), and therefore  $p = \frac{1}{2} d^2$  in (3). However, we shall retain  $g$  in the analysis as a reminder of how the physics gives structure to the theory. To plot many of the plane curves and surfaces in three dimensions which we exhibit, we choose  $g = 1$  so that dimensional variables can be displayed on the axes as a reminder of the physics (for example, (3) is then again  $p = \frac{1}{2} d^2$ ). Exactly the same diagrams will then apply if dimensionless variables are subsequently required on the axes. For example, if  $\delta$  is a reference depth (such as that on one side of a bore, as we choose in §5), then with dimensionless depth  $x = d/\delta$  and mean pressure  $y = p/g\delta^2$ , (3) becomes  $y = \frac{1}{2} x^2$ .

The hydrostatic approximation is consistent with lowest order shallow water theory (Stoker, 1957, p.30) in which the vertical velocity is zero and the horizontal velocity components are functions  $u_1(x_1, x_2, t)$  and  $u_2(x_1, x_2, t)$  which are independent of  $x_3$ .

Equation (3) is valid in any motion with these properties.

### 3. Constitutive Surfaces

A constitutive property of a particle, in any continuum, is any intrinsic property associated with the particle which holds throughout any motion whatever. Thermodynamical properties of a gas particle, such as equations of "state", provide examples; they are hypothesized before any balance equations of mass, momentum and energy are set down. Constitutive properties of a continuum therefore hold irrespective of whether these balance equations are satisfied.

Constitutive surfaces are geometrical representations of constitutive properties. Sewell and Porter (1980) introduced the term and exhibited many new examples, in compressible gas dynamics, and in shallow water theory applied to channel flow. These constitutive surfaces contain singularities associated with the cusp and swallowtail catastrophes (see also Sewell, 1987, §5.3). The present paper extends this viewpoint. There is much that can be deduced, and displayed geometrically, about the properties of a particle before the balance equations of motion are considered. At any time in its motion, each particle can be represented by a point on each constitutive surface. When the balance laws are applied, actual motions are therefore representable by tracks on the constitutive surfaces. Such motions might be steady or unsteady, and with or without discontinuities such as shocks or bores.

The properties of a particle on a streamline offer a particular example, for steady flow, of what can be deduced when only some of the balance equations are added to the constitutive properties; Sewell (1985) displayed all the 15 possible plane graphs, i.e. constitutive curves, which relate the 6 scalar variables of pressure, speed, density, mass

flow, flow stress and temperature for an ideal gas on a streamline in three dimensional flow. An actual motion will possess a particular time track, along each graph, for the pair of variables represented there.

In shallow water theory the vertical averaging process results in a situation where no distinction is made between all the actual fluid particles above the momentary  $x_1, x_2$  station. Any one of them may be regarded as the representative particle at that station. Our subsequent theory sets up a plane problem for any such representative particle, in any flow. Variables associated with the representative particle for all time include the  $p$  and  $d$  in (3), and the velocity components  $u_1$  and  $u_2$  introduced in §2. The half-parabola (3) for  $d > 0$  is therefore our first example here of a constitutive curve, in the  $p, d$  plane. Any motion of the representative particle, subsequently called simply the particle, will have a horizontal velocity vector  $\underline{u} = (u_1, u_2)$  in the  $x_1, x_2$  plane.

We define a dimensionless Froude vector

$$\underline{F} = \frac{\underline{u}}{(gd)^{1/2}} \quad \text{whose magnitude} \quad F = \frac{u}{(gd)^{1/2}} \quad (4)$$

is the standard Froude number, where  $u = |\underline{u}| \geq 0$  is the speed of the particle. Circumstances in which  $F = 1$  are called critical, with  $F > 1$  as supercritical and  $0 \leq F < 1$  as subcritical.

We now define a new variable  $h > 0$  by

$$h = \frac{1}{2} u^2 + gd \quad \text{so that} \quad d = \frac{1}{g} (h - \frac{1}{2} u^2) . \quad (5)$$

The motivation is that certain energy interpretations are associated with  $h$ , as we explain in §4. One of the most obvious, in the special case of steady flow over a flat bed, is that  $h$  then has a Bernoulli constant value along a streamline; but we shall also see in §4 how a variable similar to  $h$  is prominent in the dynamical conditions. It is best to regard  $h$  as a new variable without preconceptions, detached at the outset from such consequent particular properties, and available when the bed is uneven and the flow is unsteady. In so doing we adopt the viewpoint introduced by Sewell (1963, equation (7)) in gas dynamics, and used by Sewell and Porter (1980, equation (4.5)) in shallow water theory.

Equation (5) describes a parabolic cylinder in  $h,u,d$  space, and this is an example of a constitutive surface as defined above.

The following Theorems 1-4 are a convenient way of describing Figs. 1-4, in which the viewpoint is from the direction having colatitude  $\theta$  and longitude  $\phi$ , and in which the axes are scaled so that each represents 2 units. Each surface has one subcritical part and one supercritical part, smoothly joined along a critical space curve.

#### Theorem 1

The function

$$p(h,u) = \frac{1}{2g} \left[ \frac{1}{4} u^4 - hu^2 + h^2 \right] \quad (6)$$

obtained by inserting  $(5)_2$  into (3) describes the constitutive surface shown in Fig. 1, having the following properties.

- (i) It is saddle shaped, and strictly convex in  $h$ , everywhere.

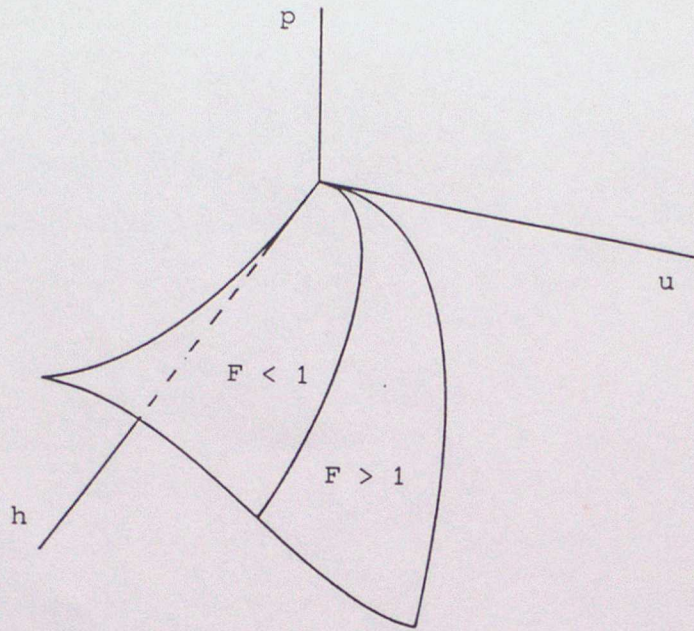


Fig. 1  $p = \frac{1}{2g} \left[ \frac{1}{4} u^4 - hu^2 + h^2 \right]$  for  $g = 1$ ,  $\theta = 30^\circ$ ,  $\phi = 20^\circ$ .

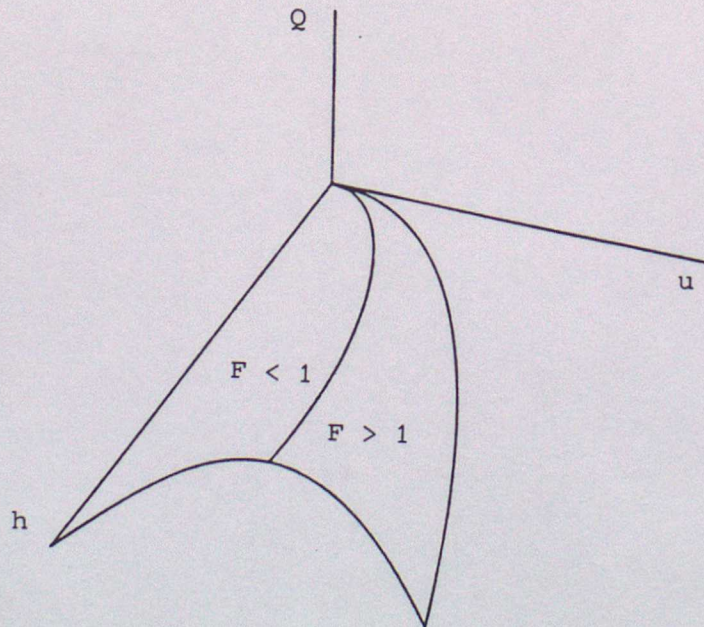


Fig. 2  $Q = \frac{1}{g} (hu - \frac{1}{2} u^3)$  for  $g = 1$ ,  $\theta = 30^\circ$ ,  $\phi = 20^\circ$ .

- (ii) Every cross-section  $h = \text{constant}$  has an inflexion where  $F = 1$ , and is strictly concave in  $u$  where  $F < 1$ , and strictly convex in  $u$  where  $F > 1$ .
- (iii) the surface lies between the parabolas  $p = h^2/2g$ ,  $u = 0$  and  $h = \frac{1}{2} u^2$ ,  $p = 0$ .

**Proof**

From (6) we find

$$\frac{\partial^2 p}{\partial h^2} = \frac{1}{g}, \quad \frac{\partial^2 p}{\partial u^2} = (F^2 - 1)d, \quad \frac{\partial^3 p}{\partial u^3} = \frac{3u}{g} \quad (7)$$

so that the determinant  $|\partial^2 p / \partial(h,u)| = -d/g < 0$ . These facts confirm (i) and (ii), and (iii) is immediate. □

Next we introduce the mass flow vector

$$\underline{Q} = \underline{u}d \quad \text{with magnitude } Q = ud \geq 0. \quad (8)$$

This  $Q$  is the vertical area of fluid which passes a horizontal station in unit time. Recalling that  $u^2 = u_1^2 + u_2^2$ , we observe that

$$\underline{Q} = -\frac{\partial p}{\partial \underline{u}} \quad \text{and} \quad Q = -\frac{\partial p}{\partial u}. \quad (9)$$

Theorem 2

The function

$$Q(h,u) = \frac{1}{g} \left[ hu - \frac{1}{2} u^3 \right] \quad (10)$$

obtained by inserting  $(5)_2$  into  $(8)_2$ , or from (6) and  $(9)_2$ , describes the constitutive surface shown in Fig. 2, having the following properties.

- (i) Every cross-section  $h = \text{constant}$  has a maximum where  $F = 1$ .
- (ii) The locus of these maxima as  $h$  varies is a space curve

$$h = \frac{3}{2} u^2, \quad Q = \frac{u^3}{g} \quad \text{implying} \quad Q = \frac{1}{g} \left[ \frac{2h}{3} \right]^{\frac{3}{2}} \quad (11)$$

which divides the surface into the subcritical and supercritical parts shown, and whose projection onto the  $Q, h$  plane is half of the bifurcation set for the cusp catastrophe.

- (iii) The surface lies between the  $h$  axis and the parabola  $h = \frac{1}{2} u^2$ ,  $Q = 0$ .

Proof

The formula

$$\frac{\partial Q}{\partial u} = \frac{1}{g} \left[ h - \frac{3}{2} u^2 \right] = (1 - F^2)g$$

justifies the results, when we recall the following terminology from catastrophe theory. □

The cuspid potentials are the set of polynomials

$$V(q; \alpha, \beta, \dots) = q^n + \alpha q^{n-2} + \beta q^{n-3} + \dots \quad (12)$$

in a single variable  $q$ , depending also on parameters  $\alpha, \beta, \dots$ , where  $n \geq 3$  is a positive integer. The function (6) is only a trivial

diffeomorphism of the cusp catastrophe potential  $n = 4$ . Therefore Fig. 2 is part of the familiar cusp catastrophe manifold  $\partial V/\partial q = 0$  (called the equilibrium surface by Sewell, 1966). We only require that part of it which lies in the positive octant, because all our variables are non-negative for physical reasons. The bifurcation set in the  $\alpha, \beta, \dots$  space is obtained by eliminating  $q$  from  $\partial V/\partial q = \partial^2 V/\partial q^2 = 0$ . Theorem 2 uses, in effect, the choice

$$V(u; h, Q) = p(h, u) + Qu \quad (13)$$

with  $h$  and  $Q$  treated as parameters, to make the connection with catastrophe theory.

### Theorem 3

The function

$$Q(h, d) = 2^{1/2}(h - gd)^{1/2}d, \quad (14)$$

obtained by inserting into  $(8)_2$  the positive root  $u$  from (5), describes the constitutive surface shown in Fig. 3, having the following properties.

- (i) Every cross-section  $h = \text{constant}$  has a maximum where  $F = 1$ .
- (ii) The locus of these maxima as  $h$  varies is a space curve

$$h = \frac{3gd}{2}, \quad Q = g^{1/2}d^{3/2}$$

which divides the surface into subcritical and supercritical parts oriented oppositely to those in Fig. 2.

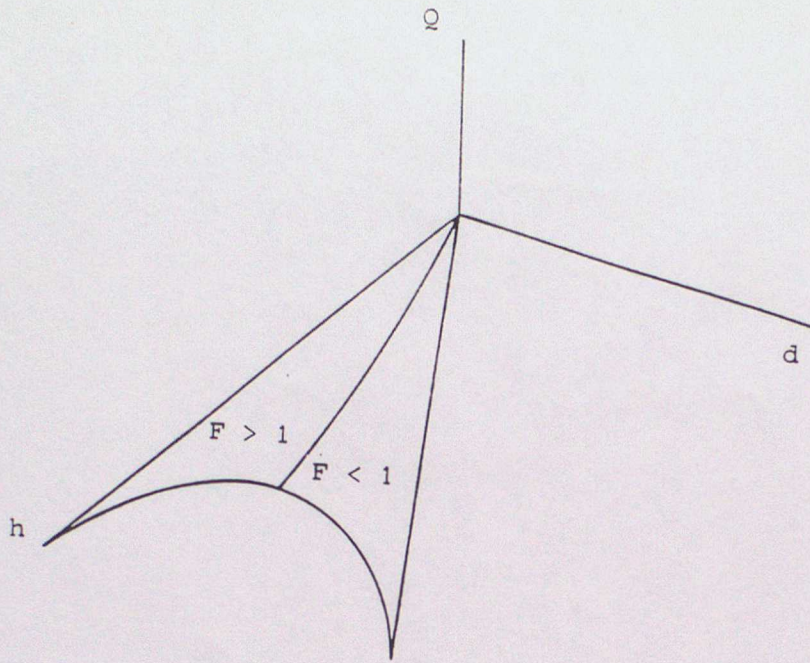


Fig. 3  $Q = (2hd^2 - 2gd^3)^{1/2}$  for  $g = 1$ ,  $\theta = 30^\circ$ ,  $\phi = 30^\circ$ .

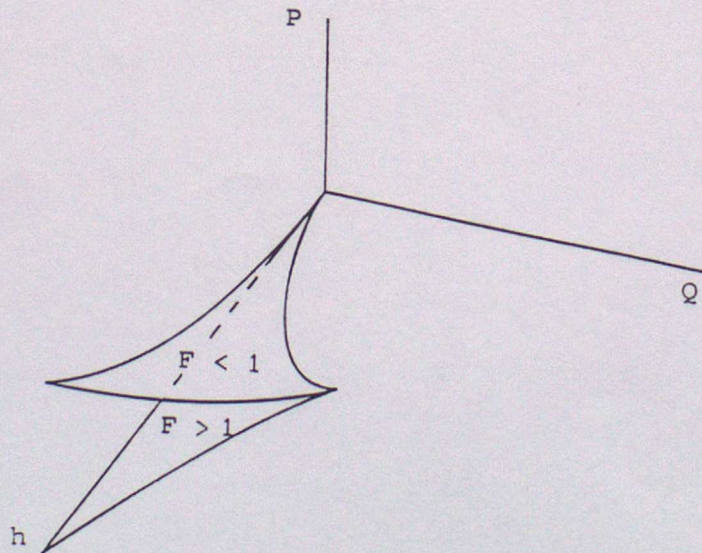


Fig. 4  $P = P(h, Q)$  for  $g = 1$ ,  $\theta = 30^\circ$ ,  $\phi = 20^\circ$ .

(iii) The surface lies between the  $h$  axis and the straight line

$$h = gd, \quad Q = 0.$$

Proof

The formulae  $u = 2^{1/2}(h - gd)^{1/2}$ ,  $\frac{h}{gd} = 1 + \frac{1}{2} F^2$  and

$$\frac{\partial Q}{\partial d} = \frac{2h - 3gd}{u} = (gd)^{1/2} \left(F - \frac{1}{F}\right)$$

justify the results. □

Consider next the  $2 \times 2$  tensor  $u_i u_j d + \delta_{ij} p$ , where  $\delta_{ij}$  is the Kronecker delta and  $i$  and  $j$  take the values 1 and 2. Its principal values are

$$u^2 d + p = P \tag{15}$$

(say) and  $p$ , with associated principal directions along and perpendicular to the local velocity vector, respectively. For this reason  $P$  is called the flow stress. The variables which become prominent in the dynamical equations of §§4 and 5 make it desirable to express  $P$  as a function  $P(h, Q)$  of  $h$  and  $Q$ . Such a function does not have a simple algebraic expression, but the important theoretical concepts of duality and the swallowtail catastrophe are introduced next to determine it graphically.

Theorem 4

The constitutive surface  $P = P(h,Q)$  has the shape shown in Fig. 4, with the following properties.

- (i) It is determined by inserting (8) and the inverse of  $(9)_2$  in (15), i.e. by a Legendre transformation of  $-p(h,u)$  with  $u$  as an active variable and  $h$  as passive.
- (ii) The surface is double valued, having a subcritical part lying above a supercritical part. The two parts join along a cusped edge where  $F = 1$ . The subcritical part is strictly jointly convex in both variables, and the supercritical part is saddle shaped but concave in each variable separately.
- (iii) The surface is part of the swallowtail bifurcation set, lying between the  $h$  axis and the parabola  $P = h^2/2g$ ,  $Q = 0$ .

Proof

- (i) The inversion of  $(9)_2$  at each given  $h$  is a function  $u(h,Q)$  which, after insertion with  $d = Q/u$  into (15), gives the function  $P(h,Q)$  with properties

$$u = \frac{\partial P}{\partial Q}, \quad P = Qu + p, \quad \frac{\partial P}{\partial h} = \frac{\partial p}{\partial h} = d \quad (16)$$

by the chain rule. These are recognizable as the standard properties of a Legendre transformation from  $-p(h,u)$  to  $P(h,Q)$ . General properties of the Legendre dual transformation are described by Sewell (1987).

- (ii) The transformation has an isolated singularity where  $F = 1$ , as  $(7)_2$  shows. The double valuedness in Fig. 4 is a consequence of

the fact that along the critical curve  $Q$  has a smooth maximum for each fixed  $h$ . Therefore the curve  $F = 1$  is a cusped edge of regression on  $P = P(h, Q)$ . The stated convexity and concavity follow from

$$\frac{\partial^2 P}{\partial h^2} = \frac{1}{(1 - F^2)g}, \quad \frac{\partial^2 P}{\partial h \partial Q} = \frac{u}{(F^2 - 1)gd}, \quad \frac{\partial^2 P}{\partial Q^2} = \frac{1}{(1 - F^2)d}$$

and the determinant  $|\partial^2 P / \partial(h, Q)| = [(1 - F^2)gd]^{-1}$ .

- (iii) The swallowtail property was shown by Sewell and Porter (1980) to follow via the more complicated gas dynamics analogue from a "ladder for the cusps" proved by Sewell (1977, 1987), that the Legendre transform of the cuspid (12) of degree  $n$  has the same shape as the bifurcation set of the cuspid of degree  $n+1$ . This is applied here for  $n = 4$ , using the fact that the bifurcation set of the cuspid of degree 5 in the  $\alpha, \beta, \gamma$  parameter space of (12) is known to have the swallowtail shape. Fig. 4 shows that part of it lying in the octant of physical interest.  $\square$

Theorem 5

- (i) The constitutive surface  $P = P(h, Q)$  in Fig. 4 has the parametric description

$$h = \frac{1}{2} u^2 + gd, \quad Q = ud, \quad P = u^2 d + \frac{1}{2} gd^2, \quad (17)$$

with  $u$  and  $d$  having the role of a pair of surface coordinates. Each coordinate curve  $u = \text{constant}$ , and  $d = \text{constant}$ , is tangential to the edge of regression.

- (ii) Each member of the family  $u = \text{constant}$  passes from  $F > 1$  to  $F < 1$  as  $d$  (and therefore  $Q$ ) increases, and appears as a straight line in plan view. Each member of the family  $d = \text{constant}$  passes from  $F < 1$  to  $F > 1$  as  $u$  (and therefore  $Q$ ) increases, and appears as a half-parabola in plan view. Each family in plan view envelops the bifurcation set  $(11)_3$ .

Proof

- (i) From (3) and (15), with  $(5)_1$  and  $(8)_2$ , we obtain (17). The edge of regression  $F = 1$  is the space curve

$$h = \frac{3}{2} u^2, \quad Q = \frac{u^3}{g}, \quad P = \frac{3u^4}{2g}.$$

The tangent to this has the direction ratios  $g : u : 2u^2$ , and this is readily verified to be the same as that of each of the two families where  $F = 1$ .

- (ii) By  $(4)_2$ , when  $u = \text{constant}$   $F$  decreases as  $d$  increases, and when  $d = \text{constant}$   $F$  increases as  $u$  increases. From (17), when  $u = \text{constant}$   $h = \frac{1}{2} u^2 + gQ/u$  is a straight line in the  $h, Q$  plane, and when  $d = \text{constant}$   $h = Q^2/2d + gd$  is a parabola.

The tangency property just proved in  $h, Q, P$  space justifies the envelope property in the  $h, Q$  plane, since  $(11)_3$  is the projection of the edge of regression onto that plane. □

Figs. 5(a) and 5(b) each display seven examples of the coordinate curves  $u = \text{constant}$  and parabolae  $d = \text{constant}$  respectively, as they appear in plan view.

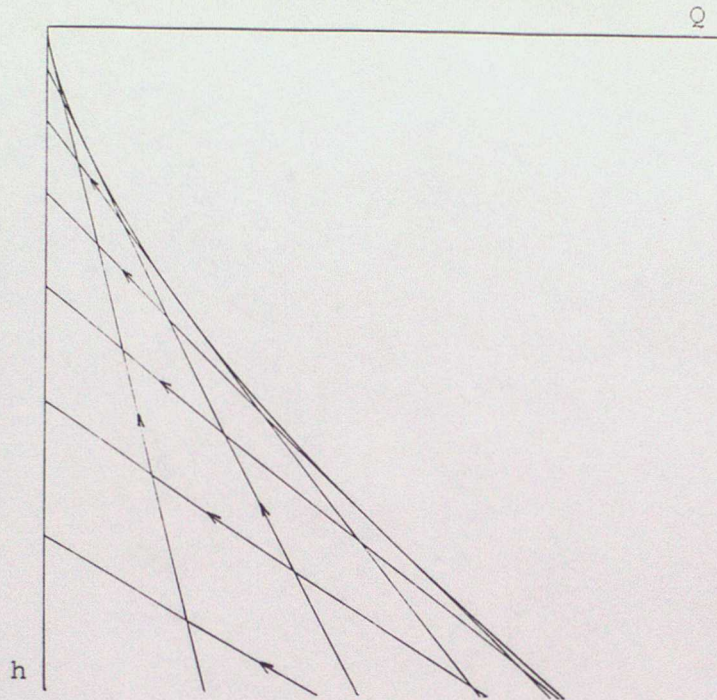


Fig. 5(a) Lines  $h = \frac{1}{2} u^2 + gQ/u$  for  $g = 1$  and constant  $u = 0.25$  (0.25) 1.75, with  $F$  increasing along arrows, and their envelope  $27g^2Q^2 = 8h^3$  where  $F = 1$ .

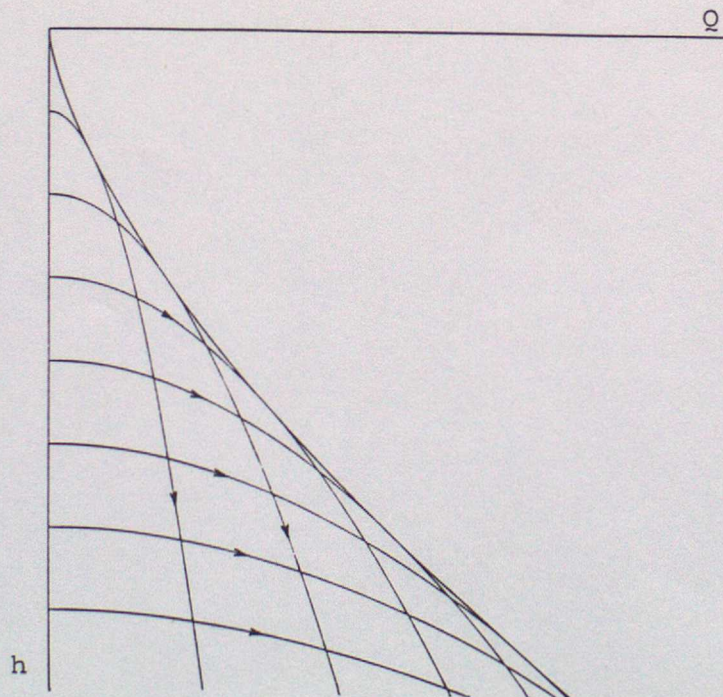


Fig. 5(b) Half-parabolaes  $h = Q^2/2d + gd$  for  $g = 1$  and constant  $d = 0.25$  (0.25) 1.75, with  $F$  increasing along arrows, and their envelope  $27g^2Q^2 = 8h^3$  where  $F = 1$ .

Each sheet of the surface in Fig. 4 will carry a coordinate grid of curves  $u = \text{constant}$  and  $d = \text{constant}$ , selected from one side of the tangency points to the envelope in Fig. 5. One can give specific examples of how a bore can be represented as an arrow from a point on either the subcritical or supercritical sheet to a point on the subcritical sheet, as we shall see in Fig. 7. The differences between the coordinate values at the two ends of the arrow is their jump at the bore.

From the viewpoint of plane mappings alone, the definitions  $(5)_1$  and  $(8)_2$  provide a single valued mapping from the positive quadrant of the  $u, d$  plane to that part of the positive quadrant of the  $h, Q$  plane which lies in the domain

$$h - \frac{3}{2} (gQ)^{2/3} \geq 0 \quad (18)$$

bounded by the bifurcation set  $(11)_3$ . The inverse mapping is double valued from inside the boundary. Figs. 2-4 display this double valuedness, not only of  $u(h, Q)$  and  $d(h, Q)$ , but also of  $P(h, Q)$  whose derivatives they are, and of the Froude number too.

It will be convenient to use  $P, u, d, F$  and  $P^*, u^*, d^*, F^*$  to denote the two sets of values which correspond to any given  $h, Q$  point satisfying the strict version of (18). One set will be subcritical and the other supercritical, but not necessarily respectively, and we refrain from specifying which, so allowing us to have either choice available. The pair of sets satisfies

$$h = \frac{1}{2} u^2 + gd = \frac{1}{2} u^{*2} + gd^* \quad , \quad Q = ud = u^*d^* \quad (19)$$

from (5)<sub>1</sub> and (8)<sub>2</sub>. Elimination of  $u$  from the first of each in (19) recovers (14), and similar elimination of  $u^*$  gives the same equation but with  $d^*$  in place of  $d$ . Put otherwise, both  $d^*/d$  and 1 are roots  $x$  of

$$x^3 - \frac{h}{gd} x^2 + \frac{Q^2}{2gd^3} = 0 .$$

From (4)<sub>2</sub> and (19) we can write this as

$$x^3 - \left[ \frac{1}{2} F^2 + 1 \right] x^2 + \frac{1}{2} F^2 = 0 .$$

This equation has roots 1 and  $\frac{1}{4} F \left[ F \pm (8 + F^2)^{1/2} \right]$ , so that

$$\frac{d^*}{d} = \frac{1}{4} F \left[ (8 + F^2)^{1/2} + F \right] , \quad \frac{u^*}{u} = \frac{1}{2F} \left[ (8 + F^2)^{1/2} - F \right] \quad (20)$$

since  $u^*/u = d/d^*$ . Therefore  $F$  and  $F^* = u^*/(gd^*)^{1/2}$  are related by

$$\frac{8}{F^*} = F^{1/2} \left[ (8 + F^2)^{1/2} + F \right]^{3/2} . \quad (21)$$

The asterisk may be transferred to the symbols without it in (20) and (21). We shall need (20) and (21) later. They are also constitutive properties, valid in the general sense described at the beginning of this Section.

Non-dimensional measures of distance from the singularity of the plane mapping  $u, d \leftrightarrow h, Q$  are  $|F - 1|$  in the  $u, d$  plane and  $G - 1$  in the  $h, Q$  plane, where

$$G = \frac{2h}{3(gQ)^{3/2}} \quad \text{and} \quad \frac{1}{2} F^{3/2} + F^{-3/2} = \frac{3}{2} G . \quad (22)$$

Equation (22)<sub>2</sub> follows by eliminating  $u$  and  $d$  from (4)<sub>2</sub>, (5)<sub>2</sub> and (8)<sub>2</sub>, and this is a constitutive curve, which we show in Fig. 6. It shows that  $F$  depends on  $h$  and  $Q$  only via the quotient  $G$ . The bifurcation set (11)<sub>3</sub> has  $G = 1$ .

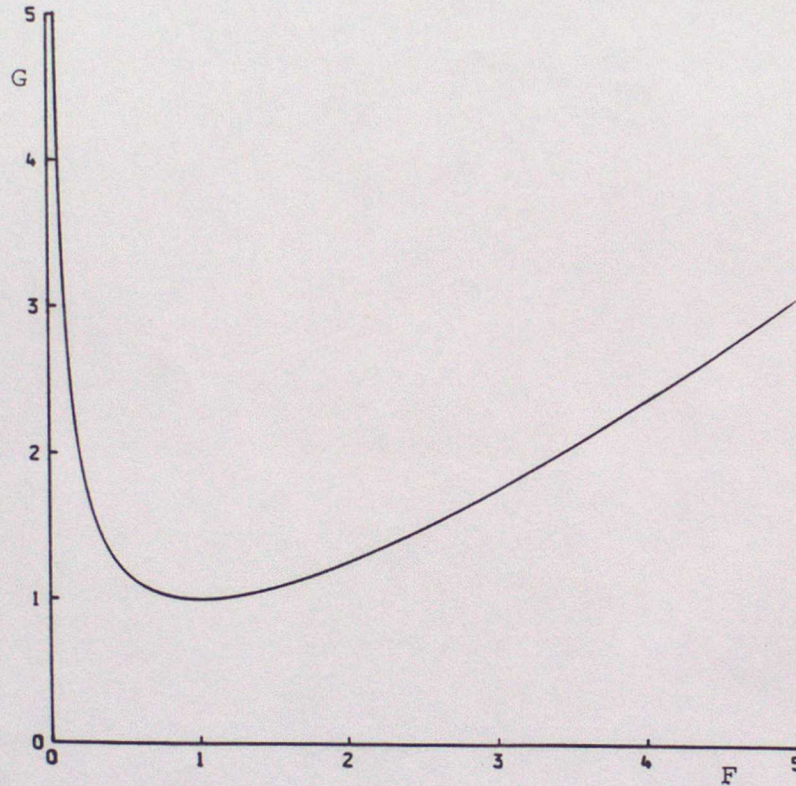


Fig. 6 Constitutive function  $G = \frac{1}{3} F^{\frac{2}{3}} + \frac{2}{3} F^{-\frac{2}{3}}$ .

We shall need another new variable  $k$  defined to be such that

$$\begin{aligned}
 g(k - b) &= h - \frac{3}{2} (gQ)^{\frac{2}{3}} \\
 &= gd \left[ \frac{1}{2} F^2 + 1 - \frac{3}{2} F^{\frac{2}{3}} \right] \\
 &= h \left( 1 - \frac{1}{G} \right) = \frac{3}{2} (gQ)^{\frac{2}{3}} (G - 1) .
 \end{aligned}
 \tag{23}$$

The non-negative expression on the right is another measure of the

distance, measured now parallel to the  $h$  axis in Fig. 5, from the bifurcation set  $(11)_3$  to an  $h, Q$  point which is constitutively admissible in the sense of (18). The expression on the left of (23) has the structure and dimensions of potential energy. Circumstances will emerge in which  $k$  can be interpreted as the maximum height available to the fluid in any continuous motion. This aspect will become prominent in the presence of an obstacle whose maximum height is  $a$ . In Part II we shall speak of free flows when  $k > a$ , and blocked flows when  $k < a$ . The distance (23) from the bifurcation set is, however, a general property available before  $a$  is introduced, and whatever be the motion.

That completes the description of those constitutive surfaces which we shall use in these papers, and we conclude this Section with an indication of the symmetric duality structure into which they and others fit, to show the connection with other investigations.

The option is available of interchanging the roles of active and passive variables in the Legendre transformation from  $-p(h,u)$  to  $P(h,Q)$  described by (6), (7),  $(9)_2$  and (16). The associated inversions of  $(16)_3$  and of  $(16)_4$  lead to another pair of Legendre dual functions which we write as

$$R(d,u) = \frac{1}{2} u^2 d + \frac{1}{2} g d^2, \quad (24)$$

$$r(d,Q) = \frac{1}{2} \frac{Q^2}{d} - \frac{1}{2} g d^2, \quad (25)$$

and whose properties are expressed in the following Theorem.

#### Theorem 6

- (i) The four functions  $p(h,u)$ ,  $P(h,Q)$ ,  $R(d,u)$  and  $r(d,Q)$  are related by Legendre transformations having the properties

$$p - P = -uQ, \quad -Q = \frac{\partial p}{\partial u}, \quad u = \frac{\partial P}{\partial Q}, \quad (26)$$

$$p + R = hd, \quad d = \frac{\partial p}{\partial h}, \quad h = \frac{\partial R}{\partial d}, \quad (27)$$

$$R + r = uQ, \quad Q = \frac{\partial R}{\partial u}, \quad u = \frac{\partial r}{\partial Q}, \quad (28)$$

$$r - P = -hd, \quad -h = \frac{\partial r}{\partial d}, \quad d = \frac{\partial P}{\partial h}. \quad (29)$$

- (ii) The transformations (27) and (28) are non-singular, and the transformations (26) and (29) have an isolated singularity where  $F = 1$ .
- (iii) The constitutive surface  $R = R(d,u)$  has a subcritical part which is jointly convex, and a supercritical part which is saddle shaped but strictly convex with respect to each of  $u$  and  $d$  separately.
- (iv) The constitutive surface  $r = r(d,Q)$  is saddle shaped everywhere. It has a subcritical part where  $r < 0$  and which is concave in  $d$  and convex in  $Q$ , and a supercritical part where  $r > 0$  which is convex in both  $d$  and  $Q$  separately. Each cross-section  $Q = \text{constant}$  has an inflexion where  $F = 1$  and  $r = 0$ , and the locus of these inflexions divides the two parts.

#### Proof

- (i) Equations (26) are available in (9) and (16). Equations (27) are readily verified from (5). Equations (28) are then verified by inverting  $Q = \partial R / \partial u$ , which is (8)<sub>2</sub>, as  $u = Q/d$  to determine (25) from (28)<sub>1</sub>. Equations (29) are then readily verified.

(ii), (iii), (iv) These properties follow from (7).

$$\frac{\partial^2 R}{\partial d^2} = g, \quad \frac{\partial^2 R}{\partial d \partial u} = u, \quad \frac{\partial^2 R}{\partial u^2} = d,$$

$$\frac{\partial^2 r}{\partial d^2} = (F^2 - 1)g, \quad \frac{\partial^3 r}{\partial d^3} = -\frac{3Q^2}{d^4}, \quad \frac{\partial^2 r}{\partial d \partial Q} = -\frac{Q}{d^2}, \quad \frac{\partial^2 r}{\partial Q^2} = \frac{1}{d}.$$

In value  $r = \frac{1}{2} (F^2 - 1)gd^2$ , and this is the only one of the four functions which can be negative. □

The analogous set of Legendre transformations in gas dynamics was given by Sewell and Porter (1980). Such quartets of transformations have been studied in general terms by Noble and Sewell (1972) and Sewell (1987). Chynoweth and Sewell (1989) gave another example in semi-geostrophic theory. Connections with variational principles were indicated by Sewell (1963, 1969, 1987).

In the special case of flows over a flat bed the function  $gR$  defined by (24) is an example of a certain hamiltonian, in a sense defined for one dimensional flows by Benjamin and Bowman (1987) in a class of problems which includes that case.

#### 4. Balance of Mass, Momentum and Energy

We now require the balance laws of mass, horizontal momentum and energy appropriate to the shallow water theory indicated in §2. As in other branches of continuum mechanics, each of these has an integral form in the first instance, which then imply either a differential equation or a jump condition depending on whether more or less continuity is assumed for the associated variables. Standard methods (see, e.g., Chadwick, 1976, Chapter 3) applied to our context lead to the balance laws which we

now quote, using some variables which the constitutive theory of §3 has highlighted.

The differential equations of mass and horizontal momentum balance, in two dimensional vector notation, are

$$\frac{\partial d}{\partial t} + \nabla \cdot \underline{Q} = 0 \quad (30)$$

and

$$\frac{\partial \underline{u}}{\partial t} + \nabla e = \underline{u} \wedge \underline{k} \omega \quad (31)$$

respectively. Here  $\nabla = (\partial/\partial x_1, \partial/\partial x_2)$ ,  $\underline{k}$  is the vertical unit vector, and

$$e = h + gb = \frac{1}{2} u^2 + gs . \quad (32)$$

When the bed is fixed  $\omega$  is the vorticity  $\partial u_2/\partial x_1 - \partial u_1/\partial x_2$ , and  $g$  is the acceleration due to gravity. When the bed is deemed to have the local vertical component of the earth's rotation,  $\omega$  is the vorticity plus that component, and the constant  $g$  also contains a centrifugal term.

From (23) we find

$$k = \frac{1}{g} \left[ e - \frac{3}{2} (gQ)^{2/3} \right] \quad \text{and} \quad b = k - (G - 1) \left( \frac{e}{g} - k \right) . \quad (33)$$

Any given bed profile function in (1) will contain the obstacle apex height  $a$  as a parameter, so that it will have the more explicit form  $b(x_1, x_2, a)$ . For consistency this must have the same value as (33)<sub>2</sub>, so that

$$b(x_1, x_2, a) = k - (G - 1) \left( \frac{e}{g} - k \right) . \quad (34)$$

This is another general constitutive relation, i.e. valid for all motions.

Whenever  $e$  and  $Q$  are given,  $k$  will be given. The right side of (33) can then be written alternatively as a single parameter function of  $F$  or  $u$  or  $d$  or  $h$ , instead of  $G$ , by using (22), (4)<sub>2</sub>, (8)<sub>2</sub> and (32)<sub>1</sub>. The maximum of each of these functions is  $k$ , when  $G = 1$  and  $F = 1$ . Comparison of the maxima  $a$  and  $k$  appearing in (34) is the starting point for our investigation of free and blocked flows in Part II. One of the alternatives to (34) is

$$b(x_1, x_2, a) = m(u) \quad \text{where} \quad m(u) = \frac{1}{g} \left( e - \frac{1}{2} u^2 \right) - \frac{Q}{u}. \quad (35)$$

For given  $e$  and  $Q$ , this describes a dependence  $u(x_1, x_2, a)$ . In the present paper we do not assume that  $e$  and  $Q$  are given.

We can regard the unknown variables in (30) and (31) as  $d$  and  $\underline{u}$ , and these equations are valid consequences of the integral balance laws provided  $d$  and  $\underline{u}$  are continuous functions of  $t, x_1, x_2$  with piecewise continuous first derivatives. In particular, this allows the bed profile function and the free surface to have a finite abrupt change in slope at isolated locations, but a vertical step in the bed is not permitted.

Energy balance warrants a more detailed discussion because of the uneven bed. It is informative to begin with an integration through the depth. The energy flux  $\rho E$  into a material volume of fluid is the rate of change of kinetic plus potential energy plus the work-rate of the boundary pressures. For a cylindrical volume bounded by the bed and the free surface, whose cross-section on the plane  $x_3 = 0$  is an area  $A$

bounded by a closed piecewise smooth curve of length  $\sigma$  with unit outward horizontal normal  $\underline{n}$ ,

$$\begin{aligned} E &= \frac{d}{dt} \iint_b^s \left[ \frac{1}{2} u^2 + gx_3 \right] dx_3 dA + \frac{1}{\rho} \iint_b^s \bar{p} \underline{n} \cdot \underline{u} dx_3 d\sigma \\ &= \frac{d}{dt} \int d \left[ \frac{1}{2} u^2 + \epsilon \right] dA + \int p \underline{n} \cdot \underline{u} d\sigma \end{aligned} \quad (36)$$

where we have used  $s = d + b$  and written

$$\epsilon = \frac{1}{2} gd + gb . \quad (37)$$

The context makes clear whether  $d$  is depth or a differential operator. This  $\epsilon$  is the net potential energy per unit mass of all the fluid particles which are momentarily above the considered location, because  $b + \frac{1}{2} d$  is the height of their centre of gravity. The analogy with thermodynamic variables in a gas identifies the function  $\epsilon(1/d, b)$  in (37) as an internal energy, where  $b$  has the formal role of an entropy (formal because  $b$  is an assigned parameter here, rather than being unspecified a priori as in a gas). The associated enthalpy function would be

$$\chi(p, b) = (2gp)^{\frac{1}{2}} + gb = gs$$

so that

$$\epsilon = \chi - p/d \quad \text{and} \quad e = \frac{1}{2} u^2 + \chi = \frac{1}{2} u^2 + \epsilon + \frac{p}{d} .$$

In that sense it would be mutually consistent to regard  $\epsilon$  as internal

energy and  $e$  as total energy = kinetic + potential + pressure energy, with the representative particle now regarded as located at the centre of gravity just mentioned.

The transport theorem applied to (36), together with (30) and (31), gives

$$E = \int (d\dot{e} + p \nabla \cdot \underline{u} - gd \underline{u} \cdot \nabla b) dA . \quad (38)$$

Both  $d/dt$  in (36) and the superposed dot in (38) denote differentiation following the particle. Since energy balance requires  $E = 0$  in a continuous flow for every  $A$ , we obtain

$$d\dot{e} + p \nabla \cdot \underline{u} - gd \underline{u} \cdot \nabla b = 0 . \quad (39)$$

Comparison of this with the standard energy balance differential equation in continuum mechanics (e.g. (3.39) of Chadwick, op. cit.) identifies the term  $g \underline{u} \cdot \nabla b$  as analogous to heat removed as if by radiation from a source within the fluid. It is evidently the rate of working of the fluid against the slope of the bed.

In fact (39) is satisfied automatically as a consequence of (30), since we have a barotropic analogue with (37) and  $p = \frac{1}{2} g d^2$  from (3).

Now suppose that each of  $d$  and  $\underline{u}$  experiences a finite discontinuity across a curve which is propagating over the  $x_1, x_2$  plane with local velocity  $C \underline{m}$ , where  $\underline{m}$  is a horizontal unit vector. In place of (30) the integral mass balance law implies the jump condition

$$[\underline{m} \cdot \underline{Q}] = C[d] . \quad (40)$$

The square bracket designates jumps, in the sense illustrated by  $[d] = d_+ - d_-$ , of values on the two sides of the curve. We define the plus and minus sides of the curve to be those into or away from which  $\underline{m}$  points, respectively. Momentum balance replaces (31) by a vector jump condition. Its  $\underline{m}$  component is

$$[(\underline{m} \cdot \underline{u})^2 d + \frac{1}{2} g d^2] = C[\underline{m} \cdot \underline{Q}] , \quad (41)$$

and its component tangential to the discontinuity requires either  $\underline{m} \cdot \underline{u} = C$  (i.e. a contact discontinuity, which the particle does not cross, which may be a shear layer or vortex sheet), or continuous tangential velocity (cf. p.118 of Chadwick, op. cit.). A finite step in the free surface is now permitted, but not in the bed function  $b(x_1, x_2)$ , which is still required to be piecewise  $C^1$ .

If the particle velocity is normal to the discontinuity on one side it must be normal on the other side, by continuity of the then zero tangential velocity. At such a place of normal transit the momentum jump conditions reduce to

$$[P] = C[\underline{m} \cdot \underline{Q}] \quad (42)$$

using (17)<sub>3</sub>.

When  $C \neq 0$  the discontinuities are said to comprise a bore, and when  $C = 0$  they comprise a hydraulic jump. The word "jump" is thus used in two different senses, general and particular, as is conventional.

It is customary to postulate that, since energy balance is not satisfied at a bore or hydraulic jump,

$$E < 0 \quad (43)$$

because of dissipative processes occurring there which are, in the strict sense, outside the realm of shallow water theory. Various expressions of (43) are derived in the next Section.

## 5. General Properties of Bores and Hydraulic Jumps

### (a) Velocity relative to the bore.

Some concise general results can be obtained by expressing the mass, momentum and energy conditions in terms of the normal fluid velocity component relative to the bore. We denote this by

$$w = \underline{m.u} - C . \quad (44)$$

### Theorem 7

We can choose  $w \geq 0$  without loss of generality, and  $w > 0$  at a bore or hydraulic jump. Neither of the latter is compatible with a contact discontinuity.

### Proof

Conditions (40) and (41) imply

$$[wd] = 0 \quad \text{and} \quad [w^2d + \frac{1}{2}gd^2] = 0 . \quad (45)$$

At a contact discontinuity  $w = 0$  by definition, and therefore  $[d] = 0$  from (45)<sub>2</sub>, so that there can be no bore or hydraulic jump. This proves the last part.

When  $w \neq 0$  a contact discontinuity is excluded, the tangential velocity must be continuous, and particles do cross a bore or hydraulic

jump. By (1) and (45)<sub>1</sub> the sign of  $w$  must be the same on both sides of the bore or jump. We can suppose  $w > 0$  henceforth, without loss of generality, since if  $-w = (-\underline{m}) \cdot \underline{u} - (-C) > 0$  we should only have to reverse the jump sign convention after (40) associated with the bore velocity  $C_{\underline{m}} = (-C)(-\underline{m})$ . □

Next we introduce the definitions

$$\tilde{h} = \frac{1}{2} w^2 + gd, \quad \tilde{Q} = wd, \quad \tilde{P} = w^2d + \frac{1}{2} gd^2 \quad (46)$$

which mimic (17), and

$$\tilde{F} = \frac{w}{(gd)^{1/2}} \quad (47)$$

which mimics the Froude number (4)<sub>2</sub>. The relation between  $\tilde{F}$  and  $F$  is

$$\tilde{F} = F \cos \theta - B, \quad \text{where} \quad B = \frac{C}{(gd)^{1/2}} \quad (48)$$

and  $\theta$  is the angle between  $\underline{m}$  and  $\underline{u}$ , so that  $\underline{m} \cdot \underline{u} = u \cos \theta$ .

### Theorem 8

- (i) There exists a constitutive surface  $\tilde{P} = P(\tilde{h}, \tilde{Q})$  shaped exactly like Fig. 4 but lying in  $\tilde{h}, \tilde{Q}, \tilde{P}$  space.
- (ii) The balance of mass and momentum and the energy loss at a bore or hydraulic jump imply that

$$[\tilde{Q}] = 0, \quad [\tilde{P}] = 0, \quad [\tilde{h}] < 0. \quad (49)$$

- (iii) Every bore or hydraulic jump can be portrayed by an arrow parallel to the  $\tilde{h}$  axis as shown in Fig. 7, i.e. from the lower sheet to the upper sheet so that

$$\tilde{F}_- > 1 \quad \text{and} \quad \tilde{F}_+ < 1. \quad (50)$$

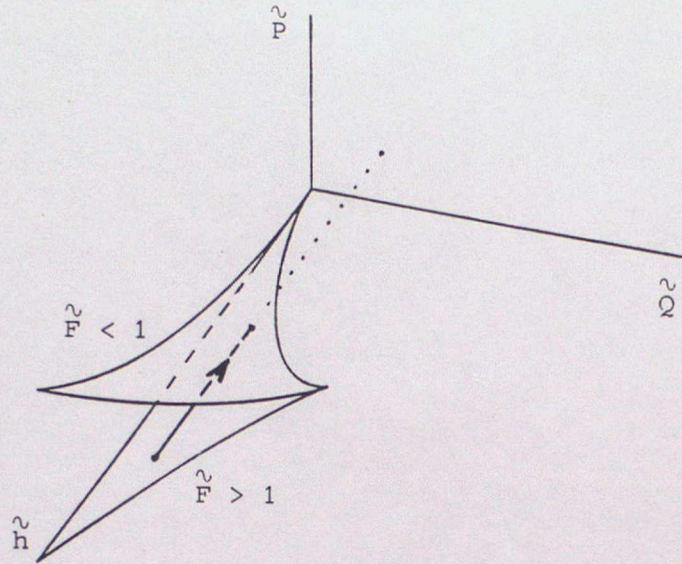


Fig. 7 Arrow representing bore or hydraulic jump from lower to upper sheet of  $\tilde{P} = P(\tilde{h}, \tilde{Q})$ , with  $g = 1$ .

(iv) Every bore or hydraulic jump has the properties

$$[w] < 0 \quad \text{and} \quad [\underline{m} \cdot \underline{u}] < 0 \quad (51)$$

and

$$[d] > 0 . \quad (52)$$

Proof

- (i) The algebraic structures of (17) and (46) are exactly the same. The trios differ only in that the parameter  $u \geq 0$  in (17) is replaced by  $w \geq 0$  in (46). Therefore the same flow stress function  $P(h, Q)$  which is parametrized by  $u$  and  $d$  in (17) can be used to describe the constitutive surface  $\tilde{P} = P(\tilde{h}, \tilde{Q})$  parametrized by  $w$  and  $d$  in (46) in  $\tilde{h}, \tilde{Q}, \tilde{P}$  space.
- (ii) When the area  $A$  in (36) is traversed by the discontinuity, the usual limiting "pill-box" argument shows that

$$E = \left[ \left( \epsilon + \frac{1}{2} u^2 \right) wd + p \underline{m} \cdot \underline{u} \right] \quad (53)$$

$$= \left[ \left( \frac{1}{2} w^2 + gd + gb \right) wd \right] + C \left[ w^2 d + \frac{1}{2} gd^2 \right] + \frac{1}{2} \left[ C^2 + (\underline{m} \wedge (\underline{u} \wedge \underline{m}))^2 wd \right] . \quad (54)$$

Mass and momentum balance imply (45), (49)<sub>1</sub>, (49)<sub>2</sub> and continuity of tangential velocity. Then, using [b] = 0 also, (54) becomes

$$E = \left[ \frac{1}{2} w^2 + gd \right] wd = [\tilde{h}] \tilde{Q} . \quad (55)$$

Here  $\tilde{Q}$  represents both values  $\tilde{Q}_+ = \tilde{Q}_-$  on either side of the discontinuity, and  $wd$  similarly by (45)<sub>1</sub>. Since  $\tilde{Q} > 0$ , we obtain (49)<sub>3</sub> from (43), (45) and (46).

(iii) The jump must be along a line with constant  $\tilde{Q}$  and  $\tilde{P}$  values, by (49)<sub>1</sub> and (49)<sub>2</sub>, i.e. parallel to the  $\tilde{h}$  axis as shown in Fig. 7. It is from the lower sheet to the upper, by (49)<sub>3</sub> and the concavity and convexity of the sheets, i.e. because  $\partial P / \partial \tilde{h} = d > 0$  and  $\partial^2 P / \partial \tilde{h}^2 = 1 / (1 - \tilde{F}^2) g$  on each sheet by (16)<sub>3</sub>. The properties (50) follow from (i).

(iv) From (50) the jump has the properties  $w_-^3 > gd_- w_- = gd_+ w_+ > w_+^3$  by (45)<sub>1</sub>, so that (51) follows. Then (52) follows from (45)<sub>1</sub> in the form

$$[w] = - \frac{w_-}{d_+} [d] = - \frac{w_+}{d_-} [d] . \quad (56)$$

□

It does not follow from (50) that every transition is from a subcritical to a supercritical flow, in the terminology introduced after (4). Instead, the next Theorem is an immediate consequence of (48).

Theorem 9

(i)  $\tilde{F} > 1$  implies

$$F > 1 \quad \text{if} \quad 0 < \cos\theta \leq B+1 ,$$

$$F < 1 \quad \text{if} \quad \cos\theta \leq B+1 < 0 .$$

(ii)  $\tilde{F} < 1$  implies

$$F < 1 \quad \text{if} \quad 0 < B+1 \leq \cos\theta ,$$

$$F > 1 \quad \text{if} \quad B+1 \leq \cos\theta < 0 .$$

(iii)  $\tilde{F} = 1$  implies  $F = \frac{B+1}{\cos\theta}$  .

(iv)  $\tilde{F} = F$  if  $\cos\theta = 1$  and  $B = 0$  ,

i.e. for normal arrival at or departure from a hydraulic jump.  $\square$

The last part means that in the case of normal transit across a hydraulic jump, the arrow on Fig. 7 is repeated in Fig. 4 in  $h, Q, P$  space. This is a graphical expression of the fact that energy loss requires the jump to be from supercritical to subcritical flow in that case.

Theorem 10

Mass and momentum balance imply that

$$E = \frac{1}{4} g[\underline{m.u}][d]^2 . \tag{57}$$

Proof

It follows from (45) and (46) that

$$[w] = -\frac{g}{2\tilde{Q}} [d^2], \quad [w^2] = -g \frac{(d_+ + d_-)^2}{2d_+d_-} [d] \quad (58)$$

and therefore from (46) and (55) that

$$[\tilde{h}] = -\frac{g}{4d_+d_-} [d]^3, \quad E = -\frac{g\tilde{Q}}{4d_+d_-} [d]^3. \quad (59)$$

From (56) and (44) with  $\tilde{Q} = w_+d_+ = w_-d_-$  we have

$$\frac{\tilde{Q}}{d_+d_-} = \frac{w_+}{d_-} = -\frac{[m \cdot u]}{[d]}, \quad (60)$$

and therefore (57) from (59). □

The formula (57) provides an alternative proof of (50) from (43), as well as having interest of its own in being a direct expression of  $E$  in terms of  $[u]$  and  $[d]$ .

#### Theorem 11

Mass and momentum balance, and energy loss, imply

$$[e] = [h] < C[m \cdot u] \quad (61)$$

at a bore or hydraulic jump.

Proof

From (3), (32), (37) and (44)

$$\left[ \epsilon + \frac{1}{2} u^2 \right] wd + p \underline{m} \cdot \underline{u} = ewd + pC \quad (62)$$

so that from (45) and (53)

$$E = \left[ e - C \underline{m} \cdot \underline{u} \right] \tilde{Q} . \quad (63)$$

The result follows from (43) since  $\tilde{Q} > 0$  and  $[b] = 0$  . □

It follows from (51) and (61) that  $[e] < 0$  if  $C \geq 0$ , but  $[e]$  can be of either sign if  $C < 0$ .

(b) Possible types of bore.

Theorem 12

Three main types of bore are possible, as shown in plan view in Fig. 8, and in a vertical cross-section containing  $\underline{m}$  in Fig. 9. They have the following properties.

(i) Particles overtake bore.

The fluid speed must be greater in the shallower water than in the deeper water, but the latter cannot be at rest or moving parallel to the bore. The shallower flow must be supercritical.

A hydraulic jump belongs to this type of bore, and has the above properties.

If there is normal transit across a hydraulic jump, the deeper flow must be subcritical, and the geometrical interpretation given after Theorem 9 applies.

(ii) Particles meet bore.

This can happen either on both sides (the deeper water could be at rest, or moving parallel to the bore); or on the shallower side only, while the bore has the same direction of travel as the  $\underline{m}$  component of the deeper water (the shallower water could be at rest, or moving parallel to the bore). The hydraulic jump of (i) can be regarded as part of the first case here.

In the first case also, if the deeper water meets the bore normally and if  $0 \geq B > -1$ , that flow is subcritical.

(iii) Bore overtakes particles on both sides.

The fluid speed must be greater in the deeper water than in the shallower water, which could be at rest or moving parallel to the bore.

#### Proof

Theorem 7 uses mass balance to justify  $\underline{m} \cdot \underline{u} > C$  on both sides of any bore or jump.

(i) A bore with  $C > 0$  is moving in the  $\underline{m}$  direction, but more slowly than particles on both sides of it. From (51) and (52)

$$\underline{m} \cdot \underline{u}_- > \underline{m} \cdot \underline{u}_+ > C \geq 0 \quad \text{with} \quad d_- < d_+ \quad (64)$$

including also a hydraulic jump ( $C = 0$ ). The speed property follows, since the tangential velocity is continuous. Also from (64),  $0 < \cos\theta_- \leq 1 \leq B_+ + 1$ , so  $F_- > 1$  from (50) and Theorem 9(i). The last property follows from (50) and Theorem 9(iv).

(ii) A bore with  $C < 0$  is moving in the direction opposite to  $\underline{m}$ , and so (by definition) will meet particles having  $\underline{m} \cdot \underline{u} \geq 0$ .

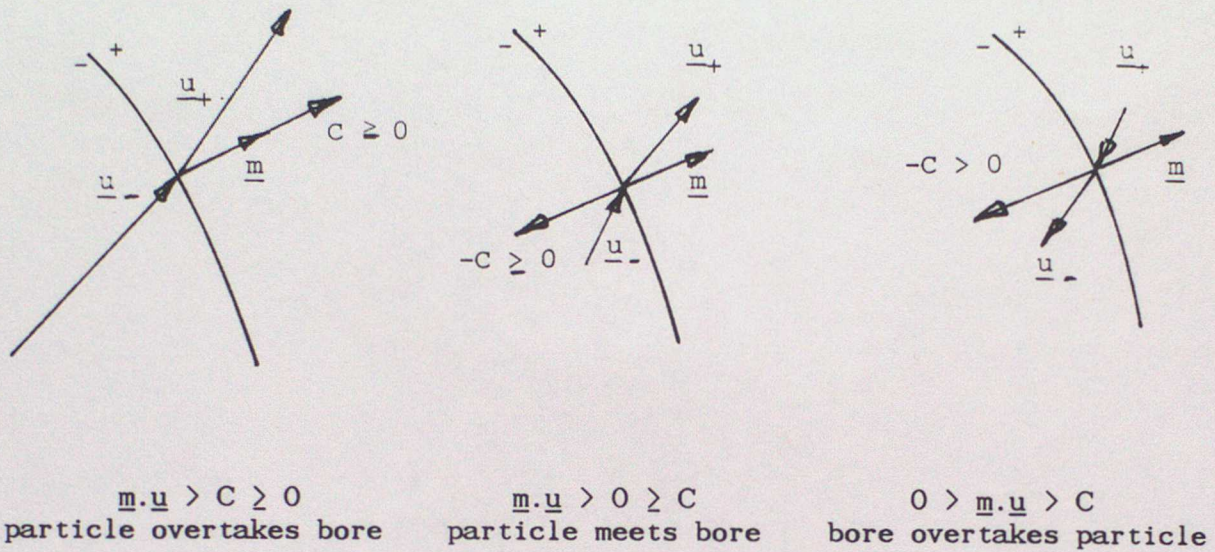


Fig. 8 . Possible bores when  $\underline{m} \cdot \underline{u} > C$ , in plan view.

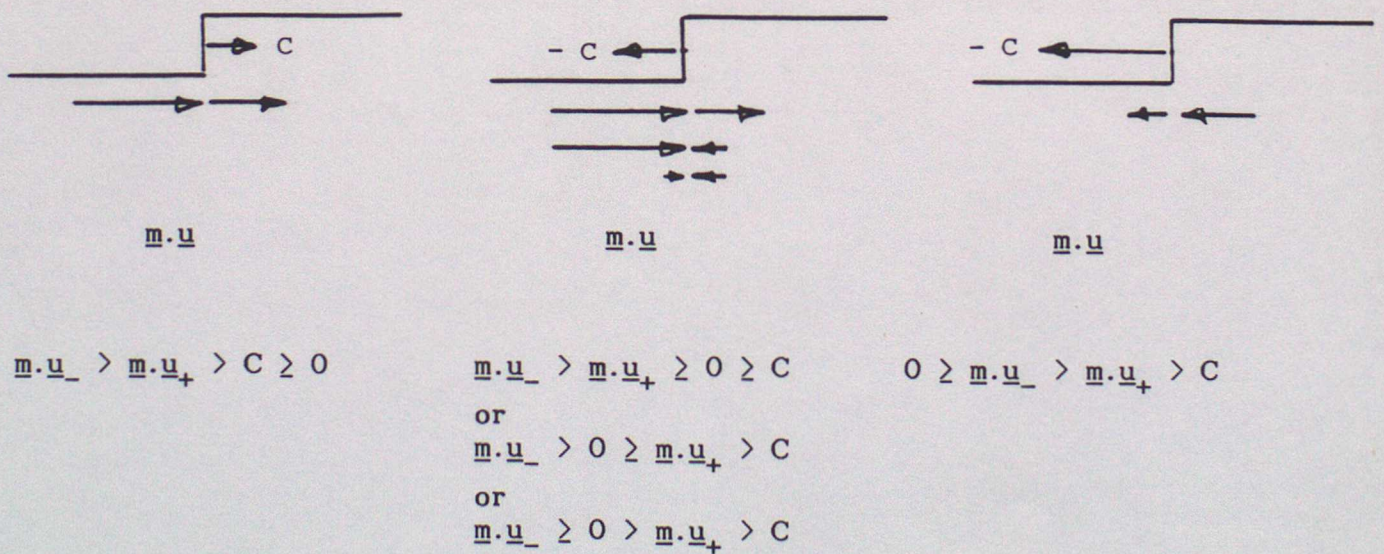


Fig. 9 Profiles of possible bores, with  $\underline{m}$  directed to the right.  
 Arrows represent the magnitudes and signs of  $\underline{m} \cdot \underline{u}$  and  $C$ .

Allowing for flow parallel to the bore (or still water), the three possible cases, all with  $d_- < d_+$ , are

$$\underline{m} \cdot \underline{u}_- > \underline{m} \cdot \underline{u}_+ \geq 0 \geq C, \quad (65)$$

$$\underline{m} \cdot \underline{u}_- > 0 \geq \underline{m} \cdot \underline{u}_+ > C, \quad (66)$$

$$\underline{m} \cdot \underline{u}_- \geq 0 > \underline{m} \cdot \underline{u}_+ > C. \quad (67)$$

The two equalities in (65) cannot occur simultaneously.

A hydraulic jump  $C = 0$  can occur in (65) if  $\underline{m} \cdot \underline{u}_+ > 0$ .

A bore cannot be such as to meet particles on the deeper side only, while moving in the same direction as the  $\underline{m}$  component of the shallower water, because this would require

$$\underline{m} \cdot \underline{u}_+ \geq 0 > \underline{m} \cdot \underline{u}_- > C \text{ which is precluded by (51) and (52).}$$

The last special property in the Theorem follows from (50) because the first hypothesis of Theorem 9(ii) is satisfied.

(iii) This is the case, also with  $d_- < d_+$ , in which

$$0 \geq \underline{m} \cdot \underline{u}_- > \underline{m} \cdot \underline{u}_+ > C. \quad (68)$$

□

The foregoing proof uses only the local properties of mass and momentum balance, and energy loss. Some features of Theorem 12 are well known, for example in one dimensional flow in a channel and over a flat bed, but the proof given here applies to any two dimensional flow in which particles cross the discontinuity, perhaps obliquely, and over an uneven piecewise  $C^1$  bed.

Evidently bores of types (ii) and (iii) may, in general, be subcritical or supercritical on either side. This is because, apart from

the special case mentioned in (ii), we cannot be sure in advance that the hypotheses of Theorem 9 are satisfied.

It may be that bores of one type are more common in nature than those of another, so that the stability of the various local types becomes an issue, in association with boundary or other conditions at a distance. Firm data is needed, and we reserve comment on this point.

(c) Solution of the jump conditions.

We now turn to the problem of expressing the properties on one side of a bore in terms of properties on the other side.

### Theorem 13

Mass and momentum balance and energy loss imply that

$$[\underline{m} \cdot \underline{u}] = - [d] g^{1/2} \left[ \frac{d_+ + d_-}{2d_+ d_-} \right]^{1/2} \quad (69)$$

and

$$C = \underline{m} \cdot \underline{u}_- - \left[ \frac{gd_+}{2d_-} (d_+ + d_-) \right]^{1/2} = \underline{m} \cdot \underline{u}_+ - \left[ \frac{gd_-}{2d_+} (d_+ + d_-) \right]^{1/2} . \quad (70)$$

Proof

Conditions (40) and (41) imply

$$[\underline{m} \cdot \underline{Q}]^2 = [d] \left[ (\underline{m} \cdot \underline{u})^2 d + \frac{1}{2} gd^2 \right]$$

which can be rearranged to give

$$[\underline{m} \cdot \underline{u}]^2 = g[d]^2 \left[ \frac{d_+ + d_-}{2d_+ d_-} \right] .$$

Then (69) follows from (51) and (52). The bore speed formulae (70) then result from inserting (69) into (40). □

We see from (69) that a knowledge of the depth on both sides of the bore is necessary and sufficient to determine  $[\underline{m.u}]$  uniquely, and therefore also to determine  $[\underline{u}]$  uniquely since the tangential component of velocity jump is zero. By inserting (69) into (57) one obtains other expressions for  $E$ , leading to (87) below.

It turns out, however, that for each particular type of bore described in Theorem 12, the depth cannot be assigned arbitrarily on both sides of the bore. Instead, the ratios of  $d_+$  and  $d_-$  which can be used in (69) are subject to definite restrictions which the following Theorems 14-17 determine. Restrictions on the corresponding bore speeds (70) are also implied.

We may say that particles arrive at the bore from the minus side if  $\underline{m.u}_- > 0$ , and from the plus side if  $\underline{m.u}_+ < 0$ . We shall regard either of these arrival sides as the known side in turn, but not both simultaneously. That is, the values of  $d$  and  $\underline{m.u}$  are regarded as given there. The other side will be the unknown side, where the restrictions on  $d$  and the consequent values of  $\underline{m.u}$  are to be found. To express properties on the unknown side in terms of those on the known side, we nondimensionalize (69) with respect to the known side, in the two cases, as follows.

We define nondimensional variables  $\lambda$  and  $\mu$  on the unknown side by the following expressions. The ratio  $\lambda$  is called the strength of the bore or hydraulic jump.

$$\lambda = \begin{cases} \frac{d_+}{d_-} \\ \frac{d_-}{d_+} \end{cases} \quad \text{and} \quad \frac{\mu}{\lambda} = \begin{cases} \frac{\underline{m} \cdot \underline{u}_+}{(gd_-)^{1/2}} & \underline{m} \cdot \underline{u}_- > 0 \\ \frac{\underline{m} \cdot \underline{u}_-}{(gd_+)^{1/2}} & \underline{m} \cdot \underline{u}_+ < 0 \end{cases} \quad \text{if} \quad (71)$$

The definitions are different in the two cases, and of course are not to be used simultaneously, even when both are available as for bores of type (ii). This  $\lambda$  is the nondimensional depth on the unknown side, and the component  $\underline{m} \cdot \underline{Q}$  of the mass flow vector (8) on the unknown side becomes this  $\mu$  after nondimensionalization.

We shall need the  $\underline{m}$  component

$$\frac{\underline{m} \cdot \underline{u}}{(gd)^{1/2}} = F \cos \theta = \hat{F} \quad (\text{say}) \quad (72)$$

of the Froude vector (4)<sub>1</sub>, and its values

$$\frac{\underline{m} \cdot \underline{u}_-}{(gd_-)^{1/2}} = \hat{F}_- \quad \text{and} \quad \frac{\underline{m} \cdot \underline{u}_+}{(gd_+)^{1/2}} = \hat{F}_+$$

on each side.

#### Theorem 14

The nondimensional version of (69) is

$$\mu = \lambda \hat{F}_c - (\lambda - 1) \left[ \frac{1}{2} \lambda (\lambda + 1) \right]^{1/2} \quad (73)$$

where  $\hat{F}_c$  here denotes the supposedly given constant

$$\hat{F}_c = \begin{cases} \hat{F}_- > 0 & \text{if } \underline{m} \cdot \underline{u}_- > 0 , \\ \hat{F}_+ < 0 & \text{if } \underline{m} \cdot \underline{u}_+ < 0 . \end{cases} \quad (74)$$

and the domain of (73) is

$$\begin{aligned} \lambda > 1 & \quad \text{if} \quad \underline{m} \cdot \underline{u}_- > 0 , \\ 0 < \lambda < 1 & \quad \text{if} \quad \underline{m} \cdot \underline{u}_+ < 0 . \end{aligned} \quad (75)$$

The nondimensional version of (70) is

$$B_{\mp} = \hat{F}_c - \left[ \frac{1}{2} \lambda (\lambda + 1) \right]^{\frac{1}{2}} \quad (76)$$

where  $B_-$  and  $B_+$  are the values of (48) in the respective cases.

Proof

The proof is just a transcription of (69) and (70). As may be anticipated from the symmetry of (69), every function  $\mu(\lambda)$  in (73) belongs to the same one-parameter  $(\hat{F}_c)$  family, but is required over complementary domains (75), by (52). □

The defining properties of the different types of bores in Theorem 12, namely (64)-(68), can be expressed in the nondimensional quantities (71), as can (40) which becomes  $\mu - \hat{F}_- = B_-(\lambda-1)$  in the first case  $\underline{m} \cdot \underline{u}_- > 0$ . This transcription implies the following restrictions to

wedges, quadrants or strips in the  $\lambda, \mu$  plane. The use of (40) does not narrow regions (79)-(81).

Nondimensionalizing with respect to the minus side as the known side:

$$(64) + (40) \Rightarrow \lambda \hat{F}_- > \mu \geq \hat{F}_-, \quad \lambda > 1. \quad (77)$$

$$(65) + (40) \Rightarrow \hat{F}_- \geq \mu \geq 0, \quad \lambda > 1. \quad (78)$$

$$(66) \Rightarrow 0 \geq \mu, \quad \lambda > 1. \quad (79)$$

Nondimensionalizing with respect to the plus side as the known side:

$$(67) \Rightarrow \mu \geq 0, \quad 1 > \lambda > 0. \quad (80)$$

$$(68) \Rightarrow 0 \geq \mu > \lambda \hat{F}_+, \quad 1 > \lambda > 0. \quad (81)$$

The following result is implied.

Theorem 15

The nondimensional jump conditions, for each type of bore, are solved by that part of the curve  $\mu(\lambda)$  in (73) which lies within the region just determined. □

It remains to determine the explicit form of (73).

Theorem 16

- (i) The function  $\mu(\lambda)$  defined by (73) for all  $\lambda > 0$  and any given  $\hat{F}_c$  is concave. It has the limits  $\mu \rightarrow 0$  as  $\lambda \rightarrow 0$  and  $\mu \rightarrow -\infty$  as  $\lambda \rightarrow \infty$ . It has a single stationary maximum at  $\lambda_m$ , say, where  $\lambda_m$  increases as  $\hat{F}_c$  increases, and  $\lambda_m = 1$  when  $\hat{F}_c = 1$ . It has a single positive value  $\lambda_0$ , say, where  $\mu(\lambda_0) = 0$ , which increases as  $\hat{F}_c$  increases. In fact

$$\lambda_0 = \begin{cases} \frac{1}{3} \left[ 1 + 2 \left[ 4 + 6\hat{F}_c^2 \right]^{\frac{1}{2}} \cos \frac{1}{3} \psi \right] & \text{if } \hat{F}_c > 0, \\ 1 & \text{if } \hat{F}_c = 0, \\ \frac{1}{3} \left[ 1 + 2 \left[ 4 + 6\hat{F}_c^2 \right]^{\frac{1}{2}} \cos \left[ \frac{1}{3} \psi - \frac{2\pi}{3} \right] \right] & \text{if } \hat{F}_c < 0, \end{cases} \quad (82)$$

where  $\cos \psi = (9\hat{F}_c^2 - 8)(4 + 6\hat{F}_c^2)^{-\frac{3}{2}}$  and  $0 \leq \psi \leq \pi$ .

- (ii) The value  $\mu = \hat{F}_c$  is attained at  $\lambda = 1$  and at another value,  $\lambda_1$ , say, where

$$\lambda_1 = \frac{1}{2} \left[ (1 + 8\hat{F}_c^2)^{\frac{1}{2}} - 1 \right] > 0, \quad (83)$$

which increases as  $\hat{F}_c$  increases, and  $\lambda_1 = 1$  when  $\hat{F}_c = 1$ .

The bore speed function  $B_T(\lambda)$  in (76) is a decreasing function of  $\lambda$  which is zero at  $\lambda_1$ .

- (iii) Each branch of the cusped curve  $\mu = \pm \lambda^{\frac{3}{2}}$  intersects  $\mu = \mu(\lambda)$  once for any given  $\hat{F}_c$ . The value of  $\lambda$ ,  $\lambda_+$  say, at which  $\mu = \lambda^{\frac{3}{2}}$  and  $\mu = \mu(\lambda)$  intersect increases as  $\hat{F}_c$  increases, and  $\lambda_+ = 1$  when  $\hat{F}_c = 1$ . If  $\hat{F}_c < 1$ ,  $\lambda_1 < \lambda_m < \lambda_+ < 1$  and if  $\hat{F}_c > 1$ ,  $1 < \lambda_m < \lambda_+ < \lambda_1$ . The value of  $\lambda$ ,  $\lambda_-$  say, at which  $\mu = -\lambda^{\frac{3}{2}}$  and  $\mu = \mu(\lambda)$  intersect increases as  $\hat{F}_c$  increases, and  $\lambda_- = 1$  when  $\hat{F}_c = -1$ .

#### Proof

- (i) The gradients of (73) with respect to  $\lambda > 0$  are

$$\mu'(\lambda) = \hat{F}_c - \phi(\lambda), \quad \text{where } \phi(\lambda) = \frac{1}{2} (4\lambda^2 + \lambda - 1)(2\lambda^2 + 2\lambda)^{-\frac{1}{2}}$$

and

$$\mu''(\lambda) = -\frac{1}{2}(8\lambda^3 + 12\lambda^2 + 3\lambda + 1)(2\lambda^2 + 2\lambda)^{-\frac{3}{2}},$$

which establishes the concavity of  $\mu(\lambda)$ .

The function  $\phi(\lambda)$  is such that  $\phi(\lambda) \sim -\frac{1}{2}(2\lambda)^{-1/2}$  as  $\lambda \rightarrow 0$ ,  $\phi(1) = 1$ ,  $\phi(\lambda) \sim \sqrt{2}\lambda$  as  $\lambda \rightarrow \infty$  and  $\phi'(\lambda) > 0$ . Since  $\mu'(\lambda) = 0$  implies  $\phi(\lambda) = \hat{F}_c$  it follows that  $\mu(\lambda)$  has a stationary point,  $\lambda_m$ , for each  $\hat{F}_c$ , having the stated properties.

A similar argument shows that  $\mu(\lambda)$  has a zero  $\lambda_0 > 0$  which increases as  $\hat{F}_c$  increases, and  $\lambda_0 = 1$  when  $\hat{F}_c = 0$ . The equation  $\mu(\lambda_0) = 0$  can be reduced to a cubic in  $\lambda_0$  and the given formulae for  $\lambda_0$  with  $\hat{F}_c \neq 0$  follow by standard methods.

(ii) Using (73),  $\mu = \hat{F}_c$  at  $\lambda = 1$  and where  $\hat{F}_c = (\frac{1}{2}(\lambda^2 + \lambda))^{1/2}$ , which has the non-negative root  $\lambda_1$  with the stated properties.

The fact that  $C = 0$  at  $\lambda_1$  is immediate.

(iii) The equation  $\mu(\lambda) = \pm \lambda^{3/2}$  can be written as

$$f_{\pm}(\lambda) = \hat{F}_c \tag{84}$$

where

$$f_{\pm}(\lambda) = (\lambda - 1) \left[ \frac{\lambda + 1}{2\lambda} \right]^{1/2} \pm \lambda^{1/2}.$$

Since  $f_{\pm}(\lambda) \sim - (2\lambda)^{-1/2}$  as  $\lambda \rightarrow 0$ ,  $f_{\pm}(1) = \pm 1$ ,  $f_{\pm}(\lambda) \sim \lambda\sqrt{2}$  as  $\lambda \rightarrow \infty$  and  $f_{\pm}'(\lambda) > 0$ , the roots  $\lambda_{\pm}$  of (84) increase with  $\hat{F}_c$  and  $\lambda_{\pm} = 1$  implies  $\hat{F}_c = \pm 1$  respectively.

Now note that

$$f_+(\lambda) - \phi(\lambda) = \frac{2\lambda(2\lambda+2)^{1/2} - 2\lambda^2 - \lambda - 1}{2(2\lambda^2 + 2\lambda)^{1/2}} \leq 0$$

for  $\lambda > 0$ , with equality only at  $\lambda = 1$ . Hence, using  $f_+(\lambda_+) = \hat{F}_c$ ,  $\mu'(\lambda_+) = f_+(\lambda_+) - \phi(\lambda_+) \leq 0$  with equality only for  $\lambda_+ = 1$ . Since  $\lambda_+ = 1$  implies  $\hat{F}_c = 1$ ,  $\mu'(\lambda_+) < 0$  for  $\hat{F}_c \neq 1$  and therefore  $\lambda_+ > \lambda_m$  for  $\hat{F}_c \neq 1$ .

Finally,  $\mu(\lambda_+) = \lambda_+^{3/2}$  and  $\mu(\lambda_1) = \hat{F}_c = f_+(\lambda_+)$  from which it follows that

$$\mu(\lambda_+) - \mu(\lambda_1) = (\lambda_+ - 1) \left[ \lambda_+^{1/2} - \left[ \frac{\lambda_+ + 1}{2\lambda_+} \right]^{1/2} \right] > 0$$

for  $\lambda_+ > 1$ . Hence for  $\lambda_+ > 1$ , that is, for  $\hat{F}_c > 1$ ,  $\mu(\lambda_+) > \mu(\lambda_1)$  and since  $\lambda_+ > \lambda_m$  we deduce that  $\lambda_+ > \lambda_1$  for  $\hat{F}_c > 1$ .

The remaining elements in the given inequalities follow from earlier parts of the proof. □

As Theorem 15 indicates the inequalities (77) - (81), each applying for one type of bore, select finite or infinite segments of the curve  $\mu = \mu(\lambda)$  implying a range of admissible jump sizes. The significance of the cusped curve  $\mu = \pm \lambda^{3/2}$  in Theorem 16 (iii) arises from the fact that, on the unknown side of the jump,

$$\mu = \hat{F}\lambda^{3/2} \tag{85}$$

from (71) and (72), and therefore in the two cases

$$\frac{\mu^2}{\lambda^3} = \begin{cases} \hat{F}_+^2 & \text{if } \underline{m} \cdot \underline{u}_- > 0, \\ \hat{F}_-^2 & \text{if } \underline{m} \cdot \underline{u}_+ < 0. \end{cases} \tag{86}$$

Within the cusp,  $\lambda^3 > \mu^2$ , so that on the unknown side of the jump  $|\hat{F}_\pm| < 1$  in the two cases, and outside the cusp  $|\hat{F}_\pm| > 1$ . For each bore type the value of  $\hat{F}_\pm$  on the unknown side is thus decided by the

location of the appropriate solution segment of  $\mu = \mu(\lambda)$  relative to the curve  $\mu = \pm \lambda^{\frac{3}{2}}$ . Theorem 16 permits the following deductions to be made from (77) - (81) for the solution of the jump conditions.

Examples of the various cases in Theorem 17 are plotted in Fig. 10, which shows the physically valid segments of  $\mu(\lambda)$  and  $B_{\mp}(\lambda)$  as full lines, and the nonphysical segments as dashed lines. The function  $\mu = \pm \lambda^{\frac{3}{2}}$  is also shown as a full line.

### Theorem 17

(i) Particles overtake bore.

By (77), if  $\hat{F}_- > 1$  there is a range  $\lambda_1 \geq \lambda > 1$  of solutions  $\mu(\lambda)$ , allowing  $\hat{F}_+ > 0$  to be on either side of unity. Fig. 10(a) illustrates this with  $\hat{F}_- = 4$ . With  $0 < \hat{F}_- \leq 1$  there is no solution.

(ii) Particles meet bore.

By (78), if  $\hat{F}_- > 1$  there is a range  $\lambda_0 \geq \lambda \geq \lambda_1$  of solutions. In Fig. 10(b)  $\hat{F}_- = 4$ . With  $0 < \hat{F}_- \leq 1$  there is a range  $\lambda_0 \geq \lambda > 1$  of solutions. In Figs. 10(c) and (d)  $\hat{F}_- = 1$  and 0.2 respectively. All require  $1 > \hat{F}_+ \geq 0$ .

By (79), there is a range  $\lambda \geq \lambda_0$  of solutions for every  $\hat{F}_- > 0$ . In Fig. 10(e)  $\hat{F}_- = 4$ . They allow  $\hat{F}_+ \leq 0$  to be on either side of -1.

By (80), there is a range  $1 > \lambda_0 \geq \lambda > 0$  of solutions for every  $\hat{F}_+ < 0$ . In Fig. 10(f)  $\hat{F}_+ = -0.2$ . They allow  $\hat{F}_- \geq 0$  to be on either side of unity.

(iii) Bore overtakes particles on both sides.

By (81), there is a range  $1 > \lambda \geq \lambda_0$  of solutions for every

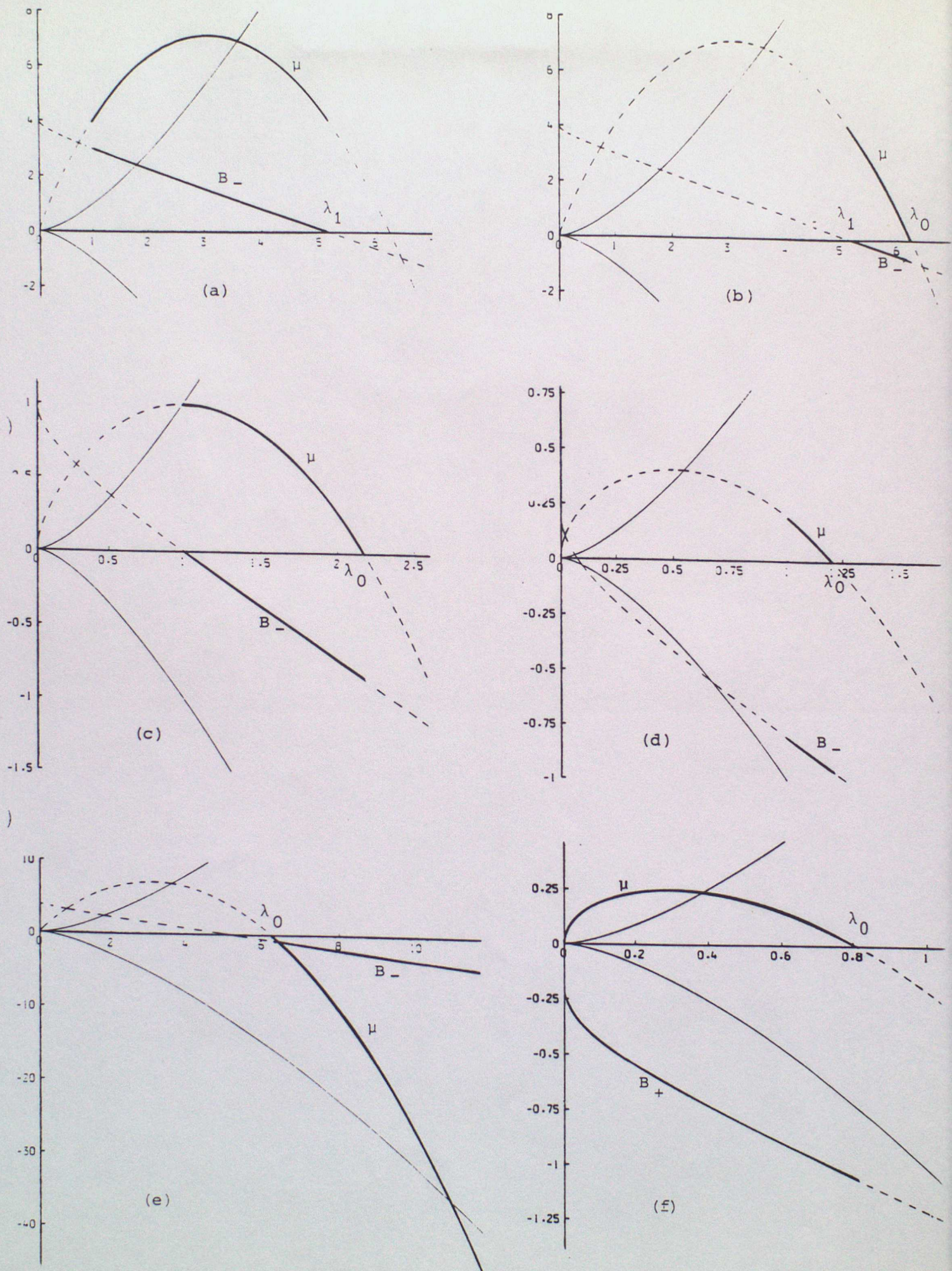


Fig. 10 Physical functions  $\mu(\lambda)$  and  $B_{\mp}(\lambda)$  (full segments) together with  $\mu = \pm \lambda^{3/2}$  (see Theorem 17).

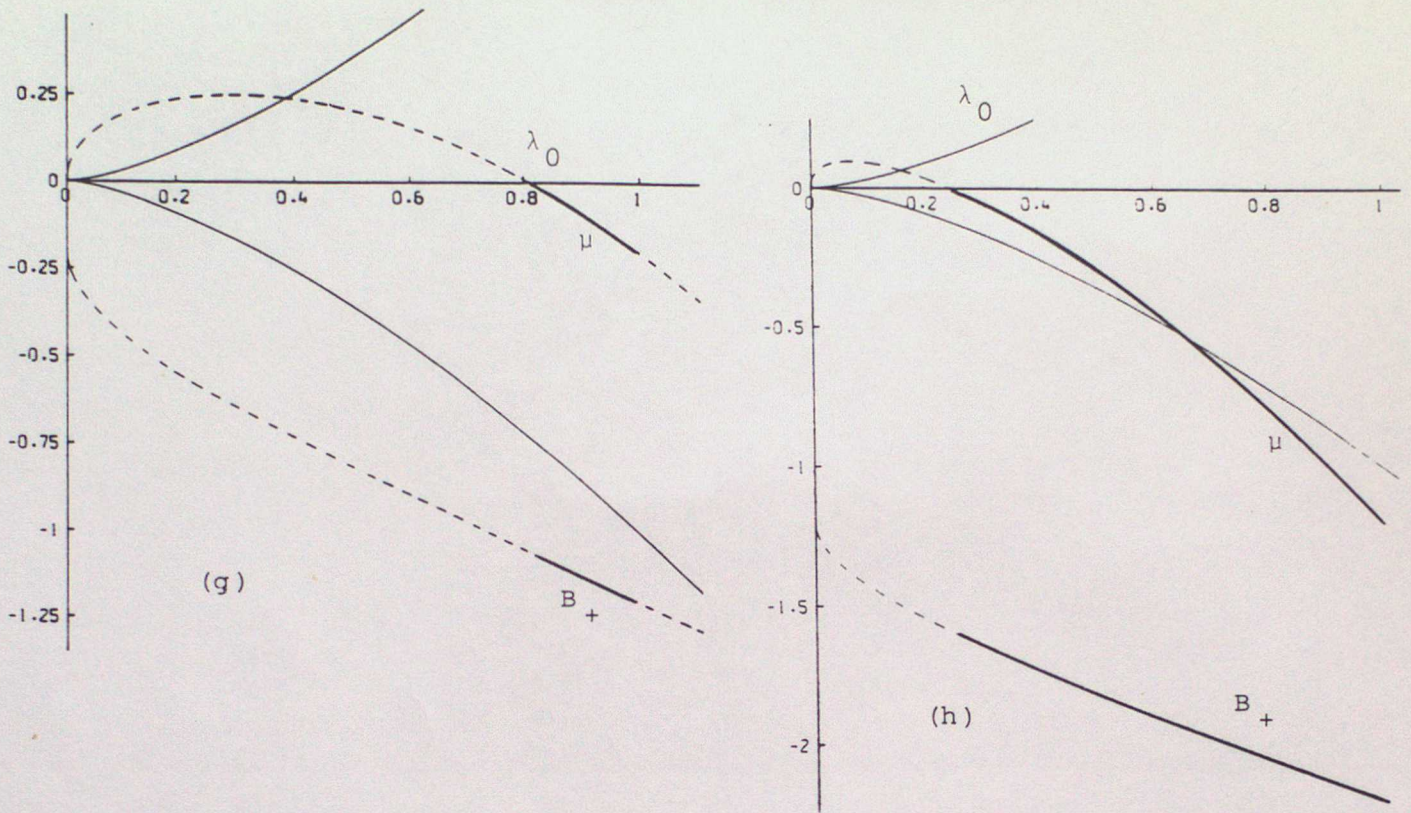


Fig. 10 Physical functions  $\mu(\lambda)$  and  $B_+(\lambda)$  (full segments) together with  $\mu = \pm \lambda^{\frac{3}{2}}$  (see Theorem 17).

$\hat{F}_+ < 0$ . If  $\hat{F}_+ < -1$  they allow  $\hat{F}_- \leq 0$  to be on either side of -1, but if  $\hat{F}_+ \geq -1$  they require  $0 \geq \hat{F}_- \geq -1$ . In Figs. 10(g) and (h)  $\hat{F}_+ = -0.2$  and  $-1.2$  respectively.

In each case there is a corresponding restricted range of bore speeds, described by (76), with the known  $\hat{F}_c$  and the range of  $\lambda$  given above. Figs. 10(a)-(e) show the function  $B_-(\lambda)$ , and Figs. 10(f)-(h) show  $B_+(\lambda)$ . □

We can summarize these results as follows. When  $\underline{m.u.} > 0$  and  $d_-$  are regarded as known, the three bores (64), (65) and (66) each have a range of possible  $d_+$  values as described by Theorem 17 with  $\lambda = d_+/d_-$ .

There are corresponding ranges of  $\underline{m} \cdot \underline{u}_+$  and  $C$  given by (69) and (70). When  $\underline{m} \cdot \underline{u}_+ < 0$  and  $d_+$  are regarded as known, the two bores (67) and (68) each have a range of possible  $d_-$  values as described by Theorem 17 with  $\lambda = d_-/d_+$ . There are corresponding ranges of  $\underline{m} \cdot \underline{u}_-$  and  $C$  given by (69) and (70).

The cusped curve  $\mu = \pm \lambda^{\frac{3}{2}}$  which discriminates between the signs of  $|\hat{F}_+| - 1$  on the unknown side of the bore in Theorem 17 is the bifurcation set associated with  $\mu$  extrema on a surface

$$v = \frac{1}{2} \left( \frac{\mu}{\lambda} \right)^2 + \lambda \quad (87)$$

in a space spanned by  $v \geq 0, \lambda \geq 0, \mu$ . This surface has the same shape as that displayed in  $h, d, Q$  space in Fig. 3 where  $\mu \geq 0$ , together with the mirror image of it in  $\mu \leq 0$ . The variable  $v$  is therefore

$$v = \begin{cases} \frac{1}{2} \frac{(\underline{m} \cdot \underline{u}_+)^2}{gd_-} + \frac{d_+}{d_-} & \text{if } \underline{m} \cdot \underline{u}_- > 0, \\ \frac{1}{2} \frac{(\underline{m} \cdot \underline{u}_-)^2}{gd_+} + \frac{d_-}{d_+} & \text{if } \underline{m} \cdot \underline{u}_+ < 0. \end{cases} \quad (88)$$

By (5) and (88),  $v$  is a nondimensional version of  $h - \frac{1}{2}(\underline{m} \wedge (\underline{u} \wedge \underline{m}))^2$ , and is  $h_+/gd_-$  or  $h_-/gd_+$  in the case of normal transit across the bore or hydraulic jump. This observation opens the way to converting the solution segments of  $\mu(\lambda)$  in (73) into other variables, by lifting the segments onto the surface (87) in Fig. 3, and then projecting them onto

other axes, and by duality into other spaces represented by, for example, Figs. 2 and 4.

By inserting (69) into (57) we find that the energy loss at a bore or hydraulic jump, when nondimensionalized according to (71), is

$$|\lambda-1|^3 \left[ \frac{\lambda+1}{\lambda} \right]^{1/2} = \begin{cases} - \left( \frac{2}{d_-} \right)^{1/2} \frac{E}{g^{1/2}} & \text{if } \underline{m} \cdot \underline{u}_- > 0, \\ - \left( \frac{2}{d_+} \right)^{1/2} \frac{E}{g^{1/2}} & \text{if } \underline{m} \cdot \underline{u}_+ < 0, \end{cases} \quad (89)$$

recalling that  $\lambda > 1$  and  $\lambda < 1$  in the two cases respectively.

In the case of normal transit the variable  $k$  defined in (23) has the properties

$$v - \frac{3}{2} \mu^{2/3} = \begin{cases} \frac{k_+ - b}{d_-} & \text{if } \underline{m} \cdot \underline{u}_- > 0, \\ \frac{k_- - b}{d_+} & \text{if } \underline{m} \cdot \underline{u}_+ < 0, \end{cases} \quad (90)$$

by (71) and (88). We make significant use of (90) in the proof of Theorem 2 of Part II.

Equations (72) and (85) show that  $\mu$  can have either sign. When  $\mu$  is used to describe a constitutive surface such as (87), in place of the non-negative  $Q$  as in (14), the geometry invites the use of  $|\hat{F}| = 1$  as the definition of criticality in place of the classical  $F = 1$  as defined after (4). It is possible to take the view that it is more natural to use the normal component  $\underline{m} \cdot \underline{u}$  of velocity rather than the absolute speed  $u$  in classifying flows as sub-critical or super-critical. Corresponding changes in certain verbal descriptions, such as some of those in Theorem 12, would need to be supplied. The

differences between the definitions disappear in the important special case of normal transit, for which  $|\underline{m} \cdot \underline{u}| = u$ , but  $\mu$  could still have either sign and  $\hat{F} = \pm F$ .

All the general properties of bores and hydraulic jumps derived in this Section apply whether or not the bed is rotating because, in contrast to (31), the spin of the bed does not appear in the general jump conditions (40), (42) and (43) which we have solved here.

#### REFERENCES

- Benjamin, T.B. and Bowman, S. 1987 *Discontinuous solutions of one-dimensional hamiltonian systems.* Proc. Roy. Soc. Lond. A413, 263-295.
- Chadwick, P. 1976 *Continuum Mechanics.* George Allen and Unwin Ltd. London.
- Chynoweth, S. and Sewell, M.J. 1989 *Dual variables in semigeostrophic theory.* Proc. Roy. Soc. Lond. A424, 155-186.
- Noble, B. and Sewell, M.J. 1972 *On dual extremum principles in applied mathematics.* J. Inst. Maths. Applics. 9, 123-193.
- Sewell, M.J. 1963 *On reciprocal variational principles for perfect fluids.* J. Math. Mech. 12, 495-504.
- Sewell, M.J. 1966 *On the connection between stability and the shape of the equilibrium surface.* J. Mech. Phys. Solids 14, 203-230.
- Sewell, M.J. 1969 *On dual extremum principles and optimization in continuum mechanics.* Phil. Trans. Roy. Soc. Lond. A265, 319-351.
- Sewell, M.J. 1977 *On Legendre transformations and elementary catastrophes.* Math. Proc. Camb. Phil. Soc. 82, 147-163.
- Sewell, M.J. 1985 *Properties of a streamline in gas flow.* Physics in Technology 16, 127-133.
- Sewell, M.J. 1987 *Maximum and Minimum Principles. A unified approach, with applications.* Cambridge University Press.
- Sewell, M.J. and Porter, D. 1980 *Constitutive surfaces in fluid mechanics.* Math. Proc. Camb. Phil. Soc. 88, 517-546.
- Stoker, J.J. 1957 *Water Waves.* Interscience, New York.